Mehrpooya, Mehdi; Taromi, Morteza; Ghorbani, Bahram

Article

Thermo-economic assessment and retrofitting of an existing electrical power plant with solar energy under different operational modes and part load conditions

Energy Reports

Provided in Cooperation with:
Elsevier

Suggested Citation: Mehrpooya, Mehdi; Taromi, Morteza; Ghorbani, Bahram (2019) : Thermo-economic assessment and retrofitting of an existing electrical power plant with solar energy under different operational modes and part load conditions, Energy Reports, ISSN 2352-4847, Elsevier, Amsterdam, Vol. 5, pp. 1137-1150, https://doi.org/10.1016/j.egyr.2019.07.014

This Version is available at:
https://hdl.handle.net/10419/243657

Energy Reports 5 (2019) 1137–1150

Contents lists available at ScienceDirect

Energy Reports

journal homepage: www.elsevier.com/locate/egyr

Research paper

Thermo-economic assessment and retrofitting of an existing electrical power plant with solar energy under different operational modes and part load conditions

Mehdi Mehrpooya [a,*], Morteza Taromi [b], Bahram Ghorbani [c]

[a] Department of Renewable Energies and Environment, Faculty of New Sciences and Technologies, University of Tehran, Tehran, Iran
[b] Department of Energy Engineering, Faculty of Environment and Energy, Science and Research Branch, Islamic Azad University, Tehran, Iran
[c] Faculty of Engineering Modern Technologies, Amol University of Special Modern Technologies, Amol, Iran

ARTICLE INFO

Article history:
Received 8 May 2019
Received in revised form 28 June 2019
Accepted 22 July 2019
Available online xxxx

Keywords:
Retrofitting
Natural gas fired power plant
Solar energy
Parabolic trough collector

ABSTRACT

This paper investigates operational modification of 250 MW Rajaee natural gas fired electrical power plant by supplying a portion of the required heat load from the solar energy source. The base case and the introduced hybrid system, both are simulated in Thermoflow and MATLAB softwares. Simulation of parabolic collector solar field in both methods of power boosting and fuel saving is performed by MATLAB. An economic analysis is done and optimal solar contribution is calculated. The obtained results specify that in solar aided electrical power generation mode can reach higher thermal efficiency in comparison with the using natural gas as fuel. In this case, with utilizing the solar field (120,000 m^2) the thermal efficiency extends from 37.0% to 39.1%. The electrical power generation by employing 7.00% of solar heat energy, up to 24.0 MW can be improved. In the fuel saving mode, the gross annual cutbacks of the fuel consumption and CO_2 emissions rates for a 12×10^4 m^2 solar collector receiver are $35{,}125\times10^3$ kg and $11{,}164\times10^3$ kg; respectively. The electrical power generation costs and fuel consumption rate saving are 80.0 US$/kWh. Also, period of return for the electrical power generation mode is six years.

1. Introduction

It is indisputable fact that conventional coal or natural gas fired power plants are the superior method for electrical power generation in the world (Hou and Hughes, 2001). However, the impact of pollutants emission on the economy, human health, and environment issues are increasingly being considered. In order to compensate for these effects, clean and sustainable energy source such as of using solar thermal energy for electrical power generation has been accepted as the efficient way (Moradi and Mehrpooya, 2017; Mehrpooya et al., 2016b). Since solar energy is unstable as well as periodic, solar electrical power generation solely, is costly (Fernández-García et al., 2010; Ashouri et al., 2015; Mehrpooya et al., 2015). A come into view technology which is known as concentrating solar power (CSP) contains considerable potential for areas with permanent sun radiation and clear sky (Mehrpooya and Sharifzadeh, 2017). The electrical power generation by CSPs covers the variable daily demand in places where air conditioning systems are mostly used (Hernández-Moro and Martínez-Duart, 2013). International Energy Agency predicated that CSPs provide about 11.3% of the world's total electrical power by 2050 (Achenbach and Riensche, 1994). From two decades ago, significant efforts have been done to integrate solar thermal energy with the fossil fuel electrical power generation plants (Mehrpooya et al., 2016a). These works along with long and short terms of sustainable development of the thermal electrical power plants which are utilizing solar thermal energy as heat source (Steinfeld and Palumbo, 2001). In this regards, an electrical power plant which consists of the existing 44 MW coal-fired and 4 MW CSP was built in Colorado (2010) (Peng et al., 2014). By integrating solar thermal energy with fossil fuel, carbon dioxide (CO_2) emission rates. Fuel costs and the sole solar system drawbacks can be decreased simultaneously (Costa, 2011). Zhao et al. (2012) propose a hybrid electrical power plant which is consisting of medium temperature solar and coal thermal energy as fuel with advantages of CO_2 capturing. In this work, the principal idea is retrofitting of a conventional electrical power plant with solar thermal energy to substitute parts of the extracted steam in the regenerative Rankin cycle (Montes et al., 2011). Ying and Hu (1999) present the solar–coal hybrid electrical power plant and calculate the thermodynamic benefits

* Corresponding author at: Department of Renewable Energies and Environment, Faculty of New Sciences and Technologies, University of Tehran, Tehran, Iran.
E-mail address: mehrpoya@ut.ac.ir (M. Mehrpooya).

https://doi.org/10.1016/j.egyr.2019.07.014

Nomenclature

a	Aperture area (m^2)
B	Day angle/ Surface tilt angle to horizontal (°)
C_p	Specific heat capacity at constant pressure (kJ/kg.°C)
D	Diameter (m)
DNI	Direct Normal Irradiance (W/m^2)
H	Enthalpy (kJ)
k	Thermal conductivity (kW/m.°C)
L	Length (m)
$\dot{m}$	Mass flow rate (kg/s)
N	Gross electrical generation (kW)
Nu	Nusselt number (-)
p	Pressure (bar)
$\dot{Q}$	Heat transfer rate (kW)
S	Absorbed heat by the solar collector (kW)
T	Temperature (°C)
W	Width (m)
$\dot{W}$	Electrical power (W)
V	Velocity (m/s)

Greek letters

η	Efficiency
Λ	Longitude angle
Ω	Hour angle
Δ	Declination angle
θ	Angle
α	Altitude angle
Φ	Latitude angle
γ	azimuth angle
Θ	Incidence angle

Subscripts

0	Atmospheric condition
A	Ambient
el	Electrical power
i	Component "i"
O	Optimum
s	Solar
se	Solar-to-electricity

Abbreviations

A	Area
B	Bled steam
CC	Combustion chamber
DEA	Deaerator
DSG	Direct Steam Generation
EC	Economizer
fw	Feed water
gen	Generator
H	Efficiency
HP	High pressure
HSPP	Hybrid Solar Power Plant

of a three stage regenerative Rankin cycle. Advantage of solar aided electrical power generation concept by energy and exergy analysis is investigated (Hu et al., 2010). The state of the working fluid is assumed unchanged with respect to indicating how working fluid can be used in different situations along with various temperatures (Kearney et al., 2003). The replacement of heaters with solar energy in different scenarios is analyzed (Popov, 2011). In this work concluded that, high pressure economizer has better performance. Some cases with (energy, exergy, environmental and economic) analysis of hybrid solar thermal electrical power plant are proposed (Suresh et al., 2010). Also, it is discussed how different kinds of replacement can have different effects on whole system performance. A more efficient way to introduce the solar electrical power in a combined cycle is preheating the combustion air in the gas turbine (Kelly et al., 2001). In this case, solar heat energy can be demonstrated in efficient way to achieve a multi-level of utilizing solar energy into conventional electrical power plants (Yang et al., 2011). The conversion efficiency of solar thermal energy to the electricity for power plant using coal as base fuel that uses low (100 °C) or medium (260 °C) solar heat energy source is 36.6% (Lewis and Nocera, 2006). The solar friction is the portion of solar thermal energy contributed towards the net electrical power output of hybrid solar power plant (HSPP) is limited. This is because of the additional cost which is caused in adapting the additional solar energy capacity. Also may not be applicable because of technical limitation of steam turbine is smaller than its specific cost (Horn et al., 2004). Thermo-economical assessment on central receiver system (CRS) integrated with hybrid solar gas turbine power plant is performed (Niknia and Yaghoubi, 2013). Similar studies on retrofitting new and existing coal-fired power plants with solar thermal energy are investigated (Niknia and Yaghoubi, 2012; Van Sciver, 2011). In the most of the proposed HSPP, effluent stream of gas turbine enters the recovery system which uses solar energy as additional source to provide required heat for bottoming cycle. The solar energy is used to achieve lower NO_x emission targets and at the same time the plant is able to attain savings in coal consumption up to 900 tons per year (Muñoz et al., 2009; Spelling et al., 0000). It is anticipated that the project will increase the electrical power plant's efficiency by up to 5.00% and will reduce CO_2 emissions by 2000 tons per year. A study is carried in direct steam generation (DSG) parabolic plant in Platform Solar de Almeria (PSA) in Spain. It is proved that, this type of plant reduces the electricity cost by 26.0% while having lower field pressure drop as compared to indirect solar systems at the same size. This would in turn, reduce the average field temperature and thermal losses which leads to higher solar field operating efficiency achieved. Unlike the DSG system, in order to reach higher operating temperature (about 600 °C), recently liquids such as molten salts are used as heat transfer fluid (HTF) have been developed. This type of HTF has greater stability against temperature in contrast with other types (Kalogirou, 2009). Although ionic liquids have mentioned advantages, but they expensive. This investment cost should be compared with other operating costs which are receiver maintenance to determine their true cost effectiveness (Giostri et al., 2012). Detail list of solar CSP and hybrid solar power plants around the world can be found in Barlev et al. (2011). In addition to the stated advantages, in a DSG hybrid solar arrangement, the used feed water in the Rankine cycle is led into the solar field and is directly heated by the incoming solar irradiation without requiring an intermediate heat exchanger. It results noticeable financial advantages and efficiency gains due to reduction of thermal and exergy losses within the system. Even though, it is in its developmental stage, the effort to integrate DSG systems with storage of thermal energy can possibly be a way forward of the future during non-solar periods of operation (Khaled, 2012). A various range of operating temperature from 60–300 °C, 100–500 °C and 150–2000 °C can be obtained by parabolic trough collector,

solar dishes and heliostat fields, respectively (Van Sciver, 2011). The process components of the Rankine cycle are steam turbine, heat exchanger, condenser and feed water pump. The heat of vaporization of the working fluid affected the efficiency of the Rankine cycle. In general, steam turbine inlet temperature values is about of 550 °C. This temperature leads Carnot efficiency about of 63.0% is obtained (Ahmadi and Dincer, 2010). The Rankine cycle can be consider as the competitive cycle for using the sun's thermal energy for electrical power generation. Among the working fluids, CO_2 is one of the most common type of working fluid due to its properties which are non-explosive, non-flammable, and naturally abundant (Chen et al., 2006). Another approach for using solar thermal energy is cogeneration system (Raj et al., 2011). The thermal efficiency of the cogeneration systems are about of 40.0–50.0% (Ahmadi and Dincer, 2010). According to the proposed description provided, using the solar thermal energy in the conventional electrical power plant has advantages in improving operating performance and decreasing costs.

In this study, retrofitted design based on the solar energy as an alternative renewable energy source for existing steam electrical power plant is done. A parabolic trough solar collector system is designed and integrated to the process. All of the required data for modeling of the solar system are developed and presented. The solar irradiation variations based on the considered climate data is shown. Retrofitted electrical power plant efficiency is calculated and effects of the key parameters such as solar fraction on the hybrid system operating performance are investigated.

2. Plant description

These days, most of the thermal electrical power plants operation is heavily dependent on fossil fuels for meeting the unceasing thirst for energy. Most of these plants, use coal as the main heat energy source for steam production in the Rankine cycle. A drastic step towards a completely renewable fuel based macro economy will certainly lead to major economic disturbance in every sect of the society. A smart decision would be the introduction of the renewable technologies in smaller doses in conjunction with the already existing fossil-based infrastructure to minimize drastic economic uncertainties.

In order to widen the pre-existing knowledge base on the hybrid coal–solar schemes, a parabolic trough solar field is aided a 250MW coal fired power unit in Abyek, Qazvin, Iran (latitude 36.2° N, longitude 50.3° E). Qazvin is an area with high solar irradiation sources. The general geographical location data is shown in Table 1. The feed water heaters are numbered in a pressure-descending order, which is currently being used in electrical power plants. The plant is constructed on 3.43 km^2 stretch of land with extensive plot remaining for expansion if solar options are considered. Its vast plane terrain is best suited to parabolic collector plants which require flat topography for deployment.

The electrical power plant is a base load type of sub-critical thermal plant. The design rate capacity will be reached to 1000 MW. In this case, it can be considered among the high-capacity power plants in Iran. The plant includes four units with the gross capacity of 250 MW at design rate conditions. Each of the units is equipped with separate generators. These generators have the ability to works up to 10.0% of the steam turbine capacity. General component specifications of electrical power plant are presented in Table 2 (Turchi and Heath, 2013).

3. System description

All the existing conventional electrical power plants which use coal or gas as fuel are the regenerative type of the Rankine steam cycle. In this kind of cycles, a part of the steam from the steam turbine is used for preheating the boiler feed water from about 70.0 °C (output stream from the condenser) to 300 °C (input stream to the economizer) (Hu et al., 2010). In this way, the Rankine steam cycle overall thermal efficiency is increased. But at the same time, the electrical power generation per unit of the input steam to the boiler is decreased. Consequently, the amount of saved steam can go through steam turbine to expands and generate more electrical power (Montes et al., 2009). As can be seen from Fig. 1, air is taken from atmosphere and pressurized by the inlet compressor. Then, it is heated by the effluent flue gas steam from economizer in the air preheater. The hot and pressurized air enters the furnace as combustion chamber (CC). In the CC, the coal as fuel is burned with the air with a ratio about of 1 to 20. The combustion product which is a high-temperature mixture of gasses is used in the evaporator as the heat source. The combusted mixture is subsequently led to the boiler evaporator section where it generates saturated vapor at 138 bar within the thick walled riser pipes without the need to return to a boiler drum. The flue gas mixture is then follows to the rest of the other heat exchangers to lose its thermal energy to the steam flowing through. The generated superheat steam with temperature and pressure of about 540 °C and bar passing through high-pressure turbine. The high pressure (HP) turbine effluent stream is divided into the two streams. A major portion of this stream enters heater at the pressure about of 33.4 bar while the other small parts are utilized in the second HP closed feed water heater as heat sources. The steam after reheating enters the medium pressure (MP) and low pressure (LP) turbines; respectively. Extractions from intermediate or exhaust pressures of each stage are made to increase the efficiency of the Rankine steam cycle. Apart from the mentioned extractions for heating in the open and closed feed water heaters, one seal steam extraction is made from the intermediate pressure turbine exhaust. The purpose of this extraction is to provide sealing for both the HP and LP ends of the turbine stages through pilot sealing so as to prevent the infiltration of low-temperature air at the lower pressure end while maintaining positive pressure at the high-pressure end during start-up. Once the turbine load is increased at its ramp rate, the sealing steam can be shut off and sealing can be provided from the high-pressure end to the low-pressure side. The LP steam turbine exhaust, along with the rest of extraction returns from the heaters, is condensed with the help of cooling water from the cooling tower.

Feed water pump subsequently raises the condenser exit pressure beyond its saturation pressure that matches the steam extraction pressure of the deaerator.

In this plant, two different categories of the feed water heater are used. Tree low pressure (LP) feed water heater which is open type is utilized before deaerator. As well as, two high pressures (HP) open types of feed water heater which are implemented to reach the temperature of the water to desired value before entering the economizer. The drain lines in between the open feed water heaters are throttled to their next heater turbine steam extraction pressure for better heat exchange. The second feed water pump is utilized to prepare the required HP turbine inlet pressure and also overcome the pressure drops in the different heat transfer sections of the boiler. The schematic process diagram of the electrical power plant with its main operating parameters is shown in Fig. 1 and Table 3; respectively.

4. Process simulation

Rankine cycles are the most used cycle in the solar aimed electrical power plant. The Rankine cycle consists of four different thermodynamic states. Heat addition and rejection at constant pressure and adiabatic reversible (isentropic) compression and

Table 1
Rajaee electrical power plant site specific geographical and climatic data.

Quantity	Unit	Value
Site Name	–	Rajaee electrical power plants
Latitude	–	50
Longitude	–	36
Average annual DNI	kWh/m^2	1300
Average annual dry bulb temperature	°C	18
Elevation	m	1360

Table 2
General specifications of Rajaee electrical power plant.

General	
Rated Plant Capacity	1000 MW
Firm Output	1850
Design efficiency at rated turbine output	37%
Average availability	93.37%
Working hours per day	24
Turbines	
Manufacturer	MHI
Type	Multi cylinder impulse reaction
Generator output	312 MVA
Speed	3000
Generator efficiency	98%
High pressure turbine isentropic efficiency	85%
Intermediate pressure turbine isentropic efficiency	91%
Low pressure turbine isentropic efficiency	85%
Boiler	
Manufacturer	IHI
Type	SR Single Drum Natural Circulation
Number	4
Generators	
Manufacturer	MHI
Rated capacity	312 MVA
Total efficiency of generator	98%

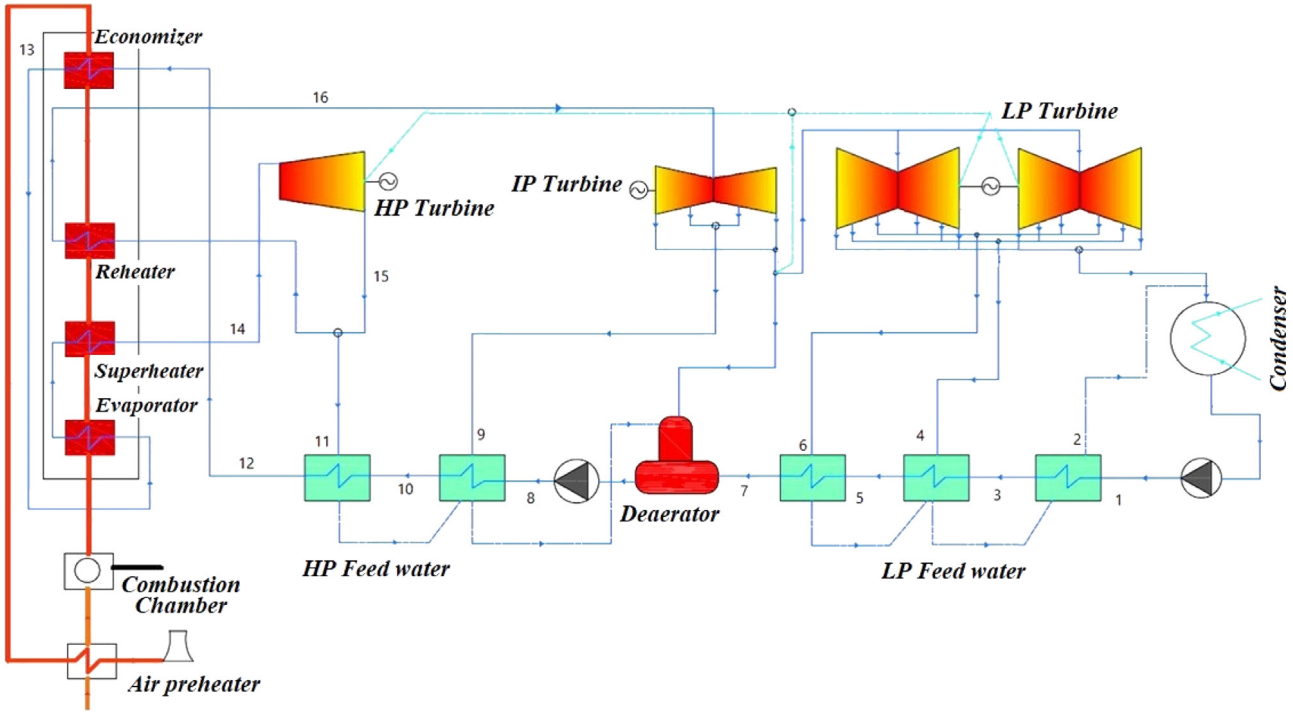

Fig. 1. Schematic process diagram of 250 MW Rajaee electrical power plant.

Table 3
Main operating parameters of the electrical power plant.

Stream number	Mass flow rate (kg/hr)	Temperature (°C)	Pressure (bar)	Enthalpy (kcal/kg)
(1)	629775	60.89	–	60.87
(2)	22256	86.45	0 .6239	629.3
(3)	629775	82.33	–	82.34
(4)	24851	148.8	1.45	661.8
(5)	629775	105.5	–	105.6
(6)	21544	209.1	2.61	689.2
(7)	629775	125	–	125.4
(8)	42754	317.1	7.40	739.2
(9)	779469	167.4	–	171.2
(10)	43553	434	17.3	794.4
(11)	779469	203.6	–	209.0
(12)	63387	349.1	37.3	740.6
(13)	779469	243.2	–	251.8
(14)	77902	538.01	140	819.3
(15)	694344	349	34.3	740.6
(16)	694344	538	34.3	844.9

expansion processes. During the heat transfer process, the working fluid phase is changed to prepare essential isothermal heat. Bu using regenerator in the Rankine cycle, the efficiency is increased due to the increasing the level of the heat transfer temperature. The reason is that the liquid is preheated before enters the vapor regenerator by using the turbine effluent stream heats. The regeneration process in the Rajaee electrical power plant is demonstrated by using some of the vapor that has partially expanded through the turbine. The extracted heat is used to preheating the pressurized liquid before entering the vapor generator. As shown in Fig. 2, in the Rajaee electrical power plant, two different types of the feed water heaters are utilized. In the open feed water heater, the pressurized liquid is preheated (2→3) by using extracted eat energy of the steam from the LP turbine at point "b". This extracted steam from the LP turbine has the same pressure with the pressurized liquid at the outlet of the pump #1. Increasing the pressure of the open feed water heater outlet liquid to the level of the vaporizer pressure is accomplished by using the pump #2 (3→4). The pressurized liquid goes through the closed feed water heater which exchanging heat is done at across the surface. In this heater, the heat of the extracted vapor from the HP turbine at point "a" is used to preheat the pressurized liquid (4→5). Unlike the prior, there is no requirement for extracted vapor and inlet pressurized liquid to being at the same pressure. The obtained liquid from the condensation of the vapor is fed back to the open feed water heater at lower pressure. Fig. 3 shows the integration of the parabolic trough collector (PTC) solar field with Rankine steam electrical power plant which uses coal as fuel. The flow rate of the produced steam depends on the solar irradiation energy from the parabolic trough collectors for heating the feed water at the economizer entrance. The economizer operates at temperatures 200.6 to 357.4 °C, so low freezing point and medium temperature operating mineral oils such as Therminol VP-1 and Hi-tech oil can be utilized as heat thermal fluid (HTF).

For times of the day when the solar irradiation energy is not available, all the feed water goes through the steam cycle by the by-pass valve. One of the constraints in the hybrid cycles is that the quality of the produced steam by using the solar irradiation energy should meet the desired requirements. Also, choosing the temperature of heat source must be higher than of the feed water or steam. Since heat energy should not be gained from the steam cycle at any section of the heat exchangers. By implementing economizer at the hybrid cycle, the temperature of the solar field is set to be 393 °C. Also, the HTF temperatures when coming back to the solar field is 290 °C to meet the above-mentioned criteria. The hybrid electrical power plant performance is affected by the solar field. So, the amount of energy consumption and the resulting economic benefit after the integration need to be analyzed. To analyze the performance of the solar field model. Fig. 4 illustrates the logic flow diagram of the used computer program.

4.1. Solar field

The PTC is a kind of solar collector that is straight in one dimension and curved as a parabola in the other two dimensions. The surface of the PTC is polished with a mirror which is fabricated by metal. The energy of solar irradiation goes through the parallel mirror symmetry planes and is focused along the focal line. The focal line is the place for heating the objects. The PTC position is aligned with the north to the south axis of the Earth and rotated to track the sun movements in the sky over the day. As another option, the PTC can be aligned on the East–west axis of the Earth. In this case, the alignment just needs to be changed during the seasons and the requirement to the tracking motors is eliminated. But, the overall efficiency of the PTC due to the cosine loss is decreased. Fig. 5 shows the considered PTC which single tracking axis.

The PTC incidence angle should be corrected because a discrepancy occurs in the higher angular incidence displacement. The discrepancy is a result of reflection and absorption losses across the receiver glass envelope. The losses have a direct relationship with incidence angles. To overcome these incremental losses in case of increasing incidence angles, the modifier of the incidence angle (Giostri et al., 2012) is utilized to rectify the discrepancy in angular displacement. A precise calculation of extraterrestrial radiation is as follow (Lanhua and L., 2012):

$$S = 24 \times 3600 \times G_{pn}/\pi \times \cos d(f_i \times \cos d(delta) \times \sin d(omigas) + 2 \times \pi \times omigas)/360^\circ \times \sin d(f_i) \times \sin d(delta) \quad (1)$$

Where S is the extraterrestrial solar radiations on a horizontal surface.

$$omigas = a\cos d(\tan d(delta) \times (-\tan d(f_i))) \quad (2)$$

Where *omigas* is the sunset hour angle.

$$delta = 23.45^\circ \times \sin d(360^\circ \times (284)/365) \quad (3)$$

where *delta* is the solar declination.

$$G_{on} = G_{sc} \times (1 + 0.033 \times \cos d(360^\circ \times n/365)) \quad (4)$$

Where G_{on} is the extraterrestrial radiation on the normal plane, f_i is the local geographical latitude (equals to 35.69°), L_{log} is the local geographical longitude (equals to 51.42°), G_{sc} is the solar

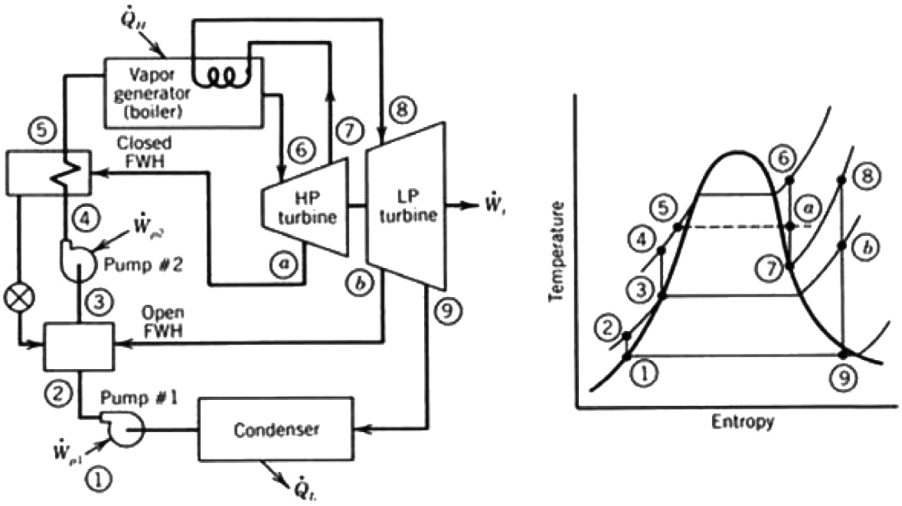

Fig. 2. Rankine cycle of the Rajaee power plant incorporating reheat and regeneration feed water heating.

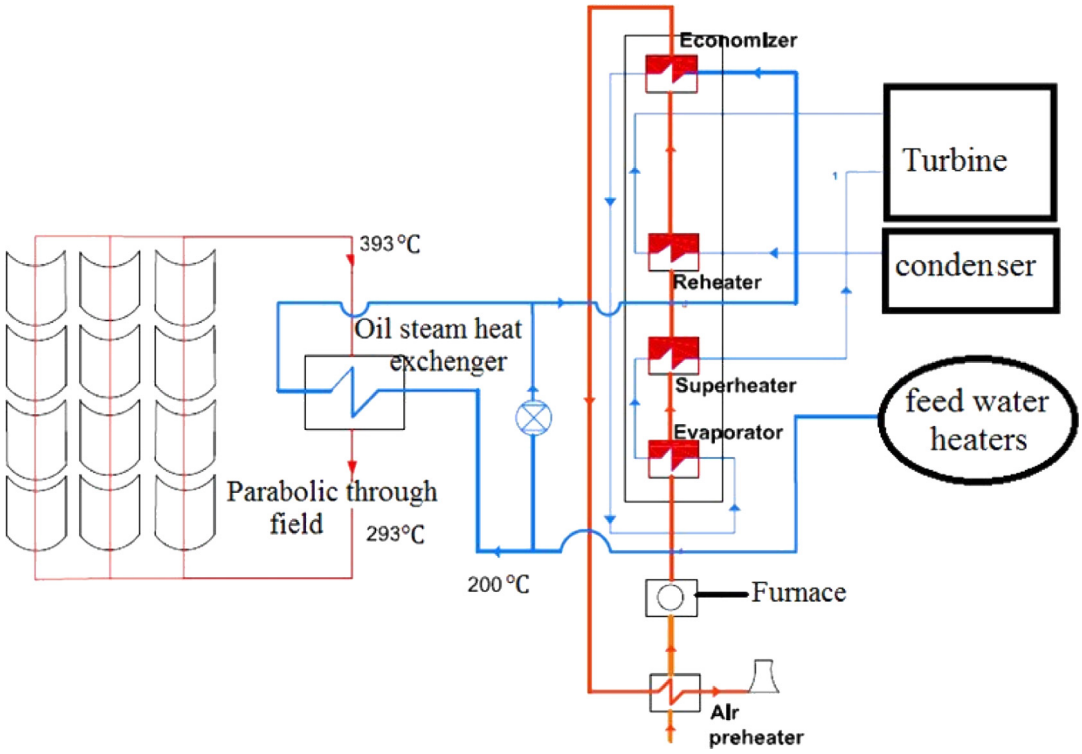

Fig. 3. Integration of the PTC solar field with the Rankine steam electrical power plant.

constant (equals to 1300 W/m^2) and is the number of day in the year.

The LS-3 is the most utilized solar collector receiver in the design of hybrid solar electrical power plants and due to its proven performance (Hong et al., 2014). The maximum operating temperature of the HTF existing from solar collector receiver is 390 °C (Shahin et al., 2016). Tables 4 and 5 illustrate the solar collector receiver geometric values and input parameters for the PTC.

These parameters were utilized to calculate model variables which are the input useful energy to the Therminol VP-1 (HTF), the collector plane temperature, the gained solar thermal energy to the collector, and solar collector receiver thermal efficiency. The gained thermal energy (useful energy) from the PTC which depends on the absorbed solar radiation incident minus losses of the solar field to the atmosphere can be calculated as follow (Soteris, 2009):

$$Q_u = F_R \times ((S \times A_a) - (A_r \times U_L \times (T_{ro} - T_o))) \quad (5)$$

Where A_a is area of the receiver (equals to 70 m^2), F_R is the heat removal factor (-), S is the absorbed heat by the solar collector receiver (kW/m^2), and U_L is the overall heat loss coefficient of the solar collector receiver (kW/m^2.°C), The area of the solar collector receiver and cover plane can be calculated as follows (Soteris, 2009):

$$A_r = \pi \times D_o \times L \quad (6)$$

$$A_G = \pi \times D_G \times L \quad (7)$$

$$A_a = (W - D_G) \times L \quad (8)$$

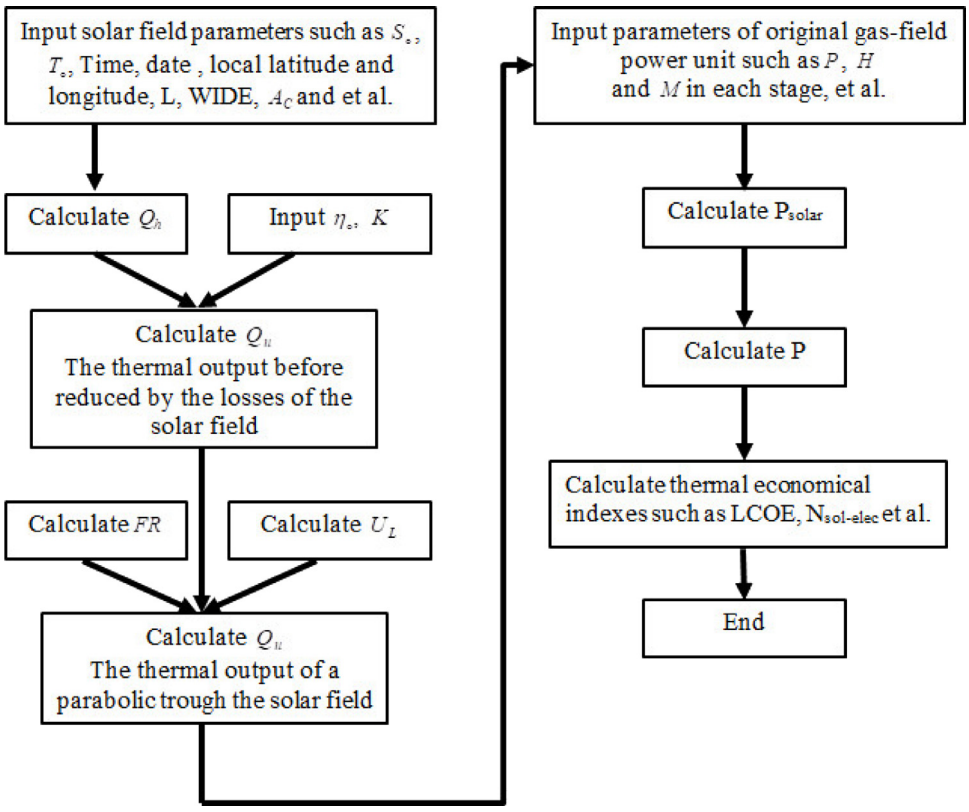

Fig. 4. Logic flow diagram of the solar field model for performance analysis.

Table 4
The LS-3 type solar collector receiver geometric values.

Parameter	Symbol	Value
Single collector width	W	5.760 (m)
Single collector length	L	12.27 (m)
Receiver inner diameter	$D_{r,i}$	0.0661 (m)
Receiver outer diameter	$D_{r,o}$	0.07 (m)
Cover inner diameter	$D_{c,i}$	0.1153 (m)
Cover outer diameter	$D_{c,o}$	0.1214 (m)
Emittance of the cover	ε_{cv}	0.86 (-)
Emittance of the receiver	ε_r	0.15 (-)
Reflectance of the mirror	ρ_c	0.94 (-)
Intercept factor	γ	0.93 (-)
Transmittance of the glass cover	τ	0.96 (-)
Absorbance of the receiver	α	0.96 (-)

Table 5
Input parameters for the performance analysis of the PTC.

Parameter	Symbol	Value
Ambient temperature	T_0	298.15 (K)
Solar irradiation	G_b	1050 (W/m^2)
Therminol VP-1 (HTF) density	ρ_c	1060 (kg/m^3)
Thermal conductivity of air	k_{air}	0.024 (W/m.K)
Thermal conductivity of HTF	k_r	0.096 (W/m.K)
Kinematic viscosity of HTF	υ_{HTF}	9.9×10^{-7} (m^2/s)
Receiver mass flow rate	$\dot{m}_r$	0.8 (kg/s)
Temperature at receiver output	T_{ro}	546.3 (K)
Temperature at receiver input	T_{ri}	493.3 (K)

Where L, W and D_o are the collector length, width and the receiver cover plane outer diameters (m); respectively (Soteris, 2009).

$$F_R = \frac{\dot{m}_{FR} \times C_P \times \left(1 - \exp\left(\frac{A_R \times U_L \times F_1}{\dot{m}_{FR} \times C_P}\right)\right)}{A_r \times U_L} \tag{9}$$

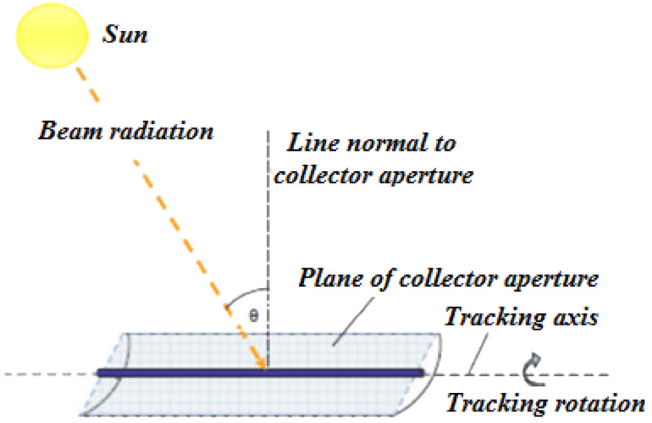

Fig. 5. The angle of incidence at the PTC aperture area (Kalogirou, 2013).

Where $\dot{m}_{FR}$ is the HTF mass flow rate (kg/s) in the solar collector receiver, C_P is the HTF specific heat capacity at constant pressure energy which can be calculated by using the average temperature of the inlet and outlet HTF temperature in the collector receiver, and F_1 is the receiver efficiency factor (-) (Soteris, 2009).

$$U_L = \frac{1}{\left(\frac{A_R}{(HCA+HRCA)\times A_G}\right) + \left(\frac{1}{HRRC}\right)} \tag{10}$$

Where HRCA is the radiation heat coefficient (kW/m^2.°C) between ambient conditions and the receiver cover planes, and can be calculated as follows (Soteris, 2009):

$$HRCA = GCE \times 5.67 \times 10^{-8} \times (T_G + T_O) \times \left(T_G{}^2 + T_O{}^2\right) \tag{11}$$

Where *GCE* represents the emittance of the cover (-). The heat coefficient radiation among the collector receiver and the cover can be calculated as follows (Soteris, 2009):

$$HRRC = \frac{5.67 \times 10^{-8} \times (T_G + T_R) \times \left({T_G}^2 + {T_{r,av}}^2\right)}{\left(\frac{1}{RE}\right) + \left(\left(\frac{A_R}{A_G}\right) \times \left(\left(\frac{1}{GCE}\right) - 1\right)\right)} \quad (12)$$

Where RE is the receiver emittance (-) and $T_{r,av}$ is the average temperature of the inlet and outlet HTF in the solar collector receiver. The receiver cover plane temperatures can be calculated as follows (Soteris, 2009):

$$T_g = \frac{(A_R \times HRRC \times T_R) + (A_G \times T_o \times (HRCA + HCA))}{(A_R \times HRRC) + (A_G \times (HRCA + HCA))} \quad (13)$$

So, the reflected solar radiation (*HRCA*), (kW) upon the collector receiver which is input heat energy in the system can be calculated as follows (Soteris, 2009):

$$HRCA = A_a \times F_R \times S \times Col_r Col_s \quad (14)$$

Where Col_r and Col_s are the total number of solar collector receiver in rows and in series, respectively. Fig. 6 compares the results of solar radiation simulation in this paper with two references (Moradi and Mehrpooya, 2017; Sabziparvar, 2008).

4.2. Boiler

The boiler is one of the main equipment in a coal-fired power plant. In this work, the boiler type and structures are not discussed in detail and just related operating parameters such as temperature, pressure, enthalpy and mass flow rate of the working fluid are considered. The coal consumption rate can be calculated by using the energy balance as follows (Hong-juan et al., 2013):

$$\dot{m}_{coal} = \frac{\dot{m}_{ms} \times (h_{ms} - h_{mw}) + \dot{m}_{rs} \times (h_{ro} - h_{ri})}{\dot{Q}_{coal} \times \eta_b} \quad (15)$$

where $\dot{m}_{coal}$ is the coal consumption rate (kg/h); $\dot{m}_{ms}$ and h_{ms} are the main stream mass flow rate (kg/h) and enthalpy (kJ/kg), respectively; h_{mw} is inlet enthalpy to the boiler (kJ/kg); m_{mrs} is the mass flow rate of the reheated steam (kg/h); h_{ro} and h_{ri} are the outlet and inlet enthalpy of the reheated steam (kJ/kg); q_{coal} is coal thermal energy (kJ/kg); η_b is the efficiency of boiler.

4.3. Turbine

In the case of replacing the extracted steam with the solar thermal energy, the steam goes through the lower stage turbines which cause steam turbine is worked working at off design conditions (Montes et al., 2009). The turbine efficiency reduction rate can be calculated by using the stream flow ratio as follows (Hong-juan et al., 2013):

$$Reduction\,(\%) = 0.191 - 0.409 \times (\dot{m}/\dot{m}_{ref}) + 0.218 \times (\dot{m}/\dot{m}_{ref})^2 \quad (16)$$

Where $\dot{m}$ is the at part load condition flow rates and $\dot{m}_{ref}$ is the design conditions flow rates. The variation of turbine efficiency is less than 1% even if the first stage extracted steam is totally replaced by the solar thermal energy. So, the steam turbine efficiency of the solar hybrid electrical power plant can be considered same as existing electrical power plant.

4.4. Feed water heaters

Extraction steam elevates inlet feed water temperatures to the boiler. Therefore, the plant thermal efficiency is increased. The adopted model for the feed water heater is described as follows (Hong-juan et al., 2013):

$$\dot{m}_{fw,i} \times \left(h_{wo,i} - h_{wi,i}\right) = \dot{m}_i \times \left(h_{i,i} - h_{d,i}\right) + \dot{m}_{d,i-1} \times \left(h_{d,i-1} - h_{d,i}\right) \quad (17)$$

where $\dot{m}_{fw,i}$ is the *i*th heater feed water mass flow rate (kg/h); $h_{wo,i}$ and $h_{wi,i}$ are the *i*th inlet and outlet heater feed water enthalpy (kJ/kg), respectively; $\dot{m}_i$ and $\dot{m}_{d,i}$ are the *i*th extracted steam and drain water flow rate of the heater (kg/h)$h_{i,i}$ and $h_{d,i}$ are *i*th the extracted steam and drain water enthalpy of heater (kJ/kg).

4.5. Deaerator

The deaerator helps purge oxygen from the feed water and controlling the corrosion. The heat balance equation is as follows (Hong-juan et al., 2013):

$$\dot{m}_{fw,o} = \dot{m}_{cond} + \dot{m}_b + \dot{m}_{fw,i} \quad (18)$$

4.6. Model evaluation

To evaluate the efficiency of the solar thermal energy utilization in the hybrid solar electrical power plant, the conversion solar heat energy to electricity efficiency (η_{se}) can be calculated as follows (Hong-juan et al., 2013):

$$\eta_{se} = \frac{1000 P_s}{\dot{Q}_{Ld}} = \frac{1000 \times \left(P_Z - \dot{Q}_b . \eta_{ref}\right)}{\dot{Q}_{Ld}} \quad (19)$$

Where P_s is output electrical power by using solar thermal energy (kW), P_Z is total output power from the hybrid solar electrical power plant (kW), $\dot{Q}_b$ is the heat load of the boiler (kW), $\dot{Q}_{Ld}$ is the direct normal irradiance focused on the collector (kW) and η_{ref} is the efficiency of reference electrical power plant which uses natural gas as fuel.

The gross value of the electrical power generation in the hybrid solar power plant can be calculated as follows (Hong-juan et al., 2013):

$$N_{solar} = \dot{Q}_{solar} \times \eta_{steam} \quad (20)$$

Where η_{steam} is the thermal efficiency of the first stage extracted steam before usage, and $\dot{Q}_{solar}$ is solar thermal energy (kW). The solar thermal energy conversion to electricity index can be calculated as follows (Hong-juan et al., 2013):

$$N_{solar} = \frac{n_{solar}}{DNI \times S} \quad (21)$$

Where *DNI* is the direct normal insolation (kW/m^2), and *S* is the aperture area of the solar collector recovers (m^2).

5. Result and discussions

The examined solar hybrid electrical power plant is situated in the northern area of Iran (Qazvin city). The electrical power plant nominal capacity is 250 MW. 225 MW of generated electrical power is sent to the grid network and the remaining 25 MW is used for the plant as the utility. As maximum capacity (rated load) of the electrical power plant is almost 250 MW, so the implemented scenarios do not impair the safety margins of the plant. The scenarios in which electrical power plant operates in fuel saving mode are safer due to this reason that the electrical power output is below the rated load value.

The simulation results in the case of maximum solar field area for both case of electrical power boosting and fuel saving mode are presented. The maximum electrical power output (power

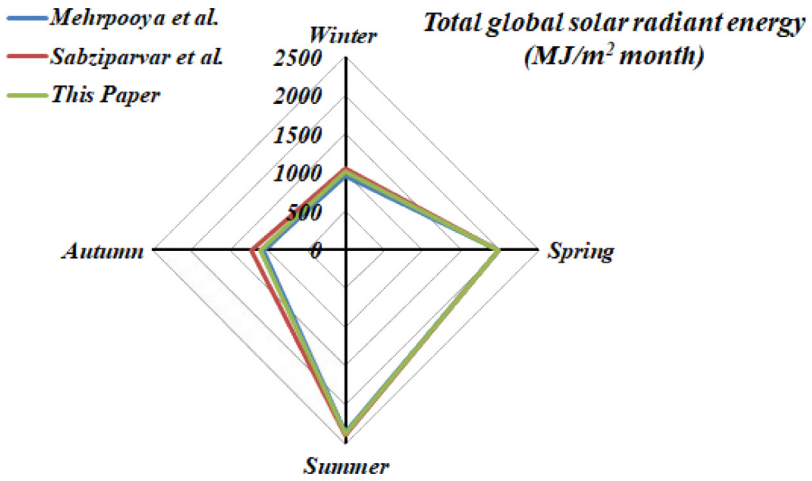

Fig. 6. Comparison of the results of solar radiation simulation in this paper with references Moradi and Mehrpooya (2017) and Sabziparvar (2008).

boosting mode) and area of the PTC solar field are 26 MW and 120,000 m^2, respectively. Thus, the total power generation of the hybrids solar electrical power plants reaches to 251 MW. The net electrical power output is 225 MW instead of 300 MW. Because, about of 7.00% of the produced electrical power (about 25 MW) is utilized as plant utility. Fig. 7 shows the variation of direct normal insolation in the Qazvin city. The hybrid solar electrical power generation mainly depends on the solar radiation rate and is affected by sun position in the sky during the day, ambient condition and velocity of the wind. High values of hybrid solar electrical power generation can be obtained when solar radiation rate and ambient temperature are high enough and wind velocity is low (between months May and August).

Fig. 8 proposes simulation results of annual electrical power generation variation with time. As can be seen, the annual electrical power generation is summation electrical power generated by the solar field and the Rankine cycle (225 MW up to 252 MW). Since the solar radiation rate is varied with time (during the day and season), the spikes points appear.

In the hybrid solar electrical power generation the saved extracted steam goes through to turbine and as result electrical power generation and the plant performance efficiency is increased. The coal fired electrical power plant efficiency is 37.0% and in the case of solar field integration, is increased to maximum value of 39.1% as shown in Fig. 8 (Hong-juan et al., 2013).

$$P = \left(\frac{\left(250 \times 10^6 + N_{solar}\right)}{\dot{m} \times LHV \times 1120} \right) \tag{22}$$

Where, P is the net electrical power output (kW), $\dot{m}$ is the mass flow rate of fuel (kg/s) and LHV is the lower heating value of fuel (kJ/kg). With the integration of solar field with the existing electrical power plant, the electrical power generation is increased (see Fig. 9), while the fuel consumption rate remains constant. The thermal electrical efficiency increases when the electrical power output overcomes the value of 225 MW.

Fig. 10 presents the percentage of solar thermal energy utilization (P_{solar}) in the hybrid solar electrical power plant. The P_{solar} can be calculated as follows (Hong-juan et al., 2013):

$$P_{solar} = \frac{\dot{Q}_{solar}}{\dot{Q}_{solar} + \dot{Q}_{boiler}} \tag{23}$$

Where $\dot{Q}_{solar}$ is the transferred solar thermal energy into the feed water heater (MW) and $\dot{Q}_{boiler}$ is the total value of the thermal energy loaded in the boiler after replacement (MW).

In the case of the fuel saving mode, the output electrical power remains constant at the value of 225 MW, while fuel consumption and CO_2 emission rates are decreased. The fuel analysis to investigate the performance of the boiler is shown in Table 6. Table 7 shows the results of fuel consumption and CO_2emissions rates for power boosting and fuel saving modes. As can be inferred, the highest fuel conservation and CO_2 emissions reduction rates are obtained for solar field area of about 120,000 m^2.

Fig. 11 shows the effect of solar irradiation rate on the energy input to the solar collector receiver. The input energy to solar collector receiver has the linear relationship with solar irradiation rate variations.

The Therminol VP-1 as HTF is used in the PTC. The HTF mass flow rate is very effective in the PTC performance. As shown in Fig. 12, by increasing the HTF mass flow rate; the gained solar thermal energy rate and the thermal efficiency of the PTC are increased.

The PTC aperture area presents the geometric properties of the solar receiver collector. It is the area where the sun shines upon and consequently reflected the receiver pipe. As Fig. 13 shows the variation of the useful thermal energy rate with increasing the solar receiver collector aperture area.

6. Economic analysis

6.1. Cost modeling and estimation for parabolic trough collector power plant

The economic analysis is done based on the performance analysis results of the hybrid solar electrical power plant results. Currently, there is not much literature available in formulating actual investment costs to help estimate the cost of PTC electrical power plants. Alternatively, there are some researches which present the various plant cost element estimates pertaining to construction and deployment of this technology for reference plants. Owing to the PTC technological maturity and its modular nature, the cost of PTC electrical power plants can be calculated with the small margin of error to the actual field cost. The required aperture area to increase the temperature of the HTF to a field outlet temperature is determined for a given solar loop based on LS-3 collector design characteristics. The energy collected from a single solar loop is subsequently used to calculate the total field aperture area for nominal solar electrical power output. The nominal aperture area is multiplied by optimum solar to ensure that longer design point of electrical power output is gained from the PTC electrical power plants (Shimeles, 2014).

$$N_{technician} = 1 + N_{personnel\text{-}tech} \times A_{PTC} \times N_{collectors} \tag{24}$$

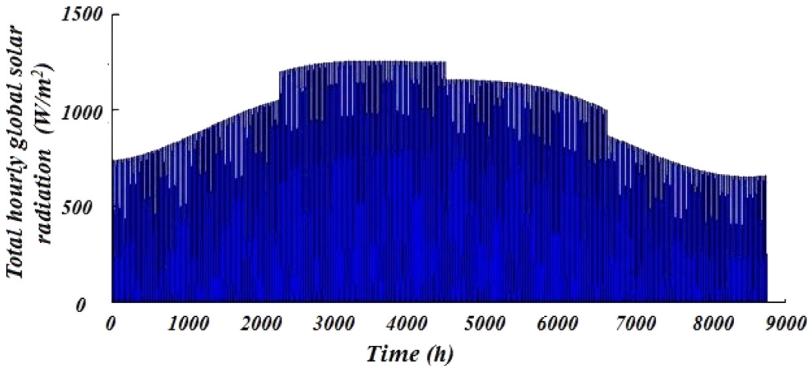

Fig. 7. Variation of direct normal insolation with time in the Qazvin city.

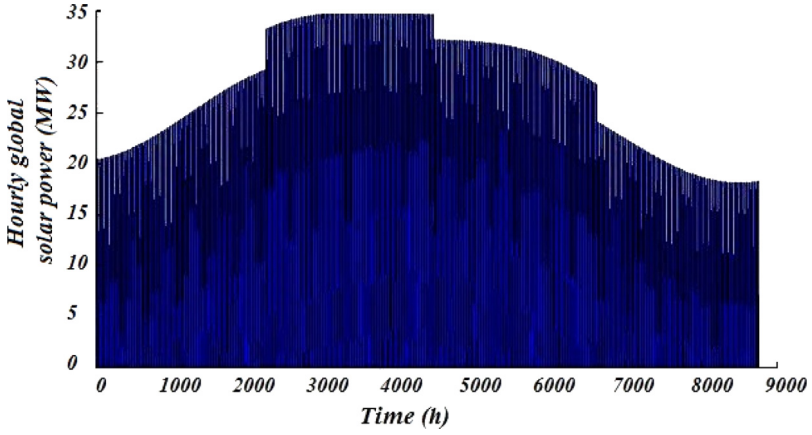

Fig. 8. Hybrid solar electrical power output variation with time.

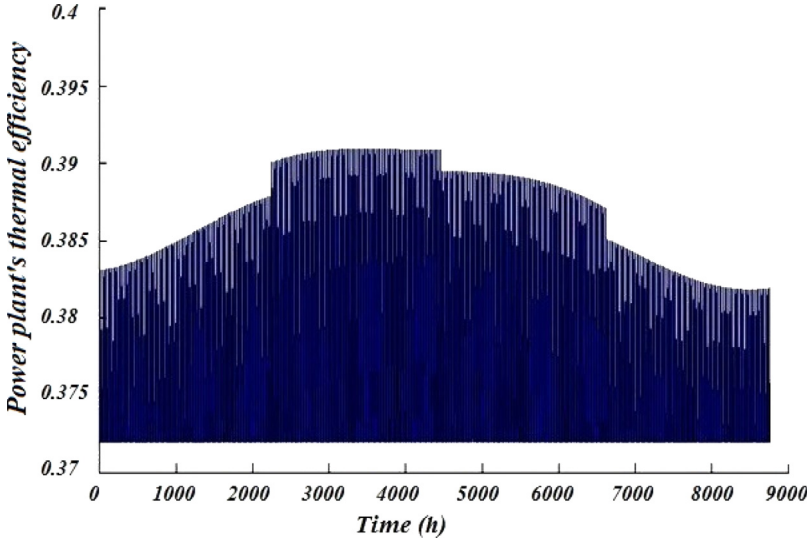

Fig. 9. Variation of electrical power plant's thermal efficiency with time.

Table 6
The electrical power boosting mode simulation results.

Total solar field area	Electrical power output (MW)	Power plant efficiency (%)	Solar thermal energy (%)
30000 m^2	234	38.11	1.98
60000 m^2	239	38.72	3.83
90000 m^2	245	39.07	5.74
120,000 m^2	251	39.44	7.53

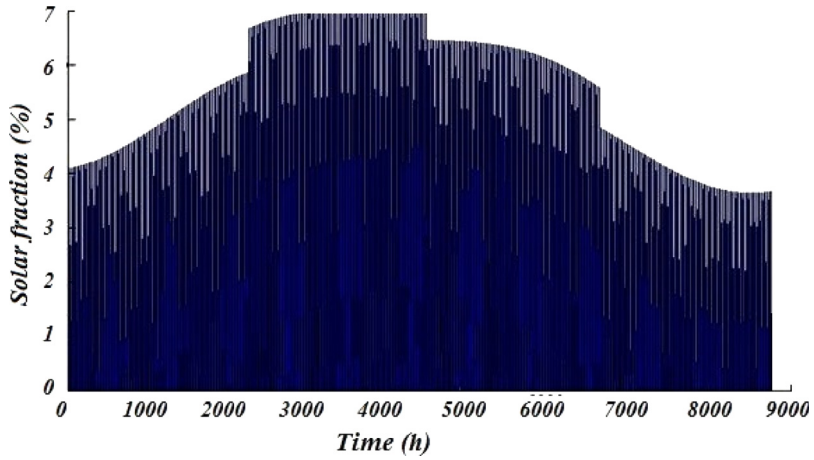

Fig. 10. Variation of solar thermal energy utilization percentage with time.

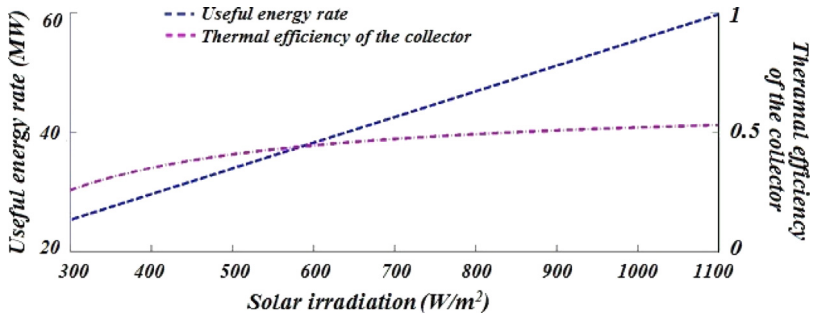

Fig. 11. Variation of the input energy to solar collector receiver and the thermal efficiency of the PTC relative to the solar irradiation.

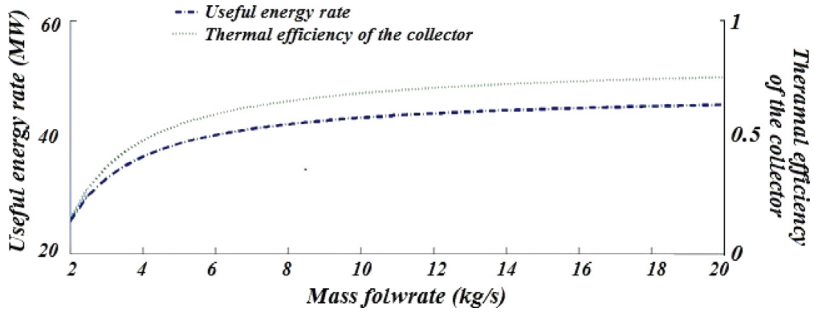

Fig. 12. Impact of HTF mass flow rate on the gained solar thermal energy rate and the thermal efficiency of the PTC.

Table 7
The fuel saving mode simulation results.

Total solar field area	Fuel consumption rate (kg/hr)	CO_2 emissions rate (kg/hr)
30000 m^2	47028	37528
60000 m^2	45994	36703
90000 m^2	44633	35617
120,000 m^2	43327	34575

$$N_{operator} = 1 + N_{personnel-oprtr} \times A_{PTC} \times N_{collectors} \quad (25)$$

Where $N_{personnel\text{-}tech}$ is number of technician per 100,000 m^2 of aperture area and $N_{personnel\text{-}oprtr}$ number of operators per 100,000 m^2 of aperture area. (See Tables 8 and 9.)

6.2. Cost modeling of the electrical power generation plant

Estimating the total capital, operating and maintenance costs are useful for providing economical comparison benchmark to every solar repower option being investigated. The fossil fuel plant is compared based on its specific fuel consumption, emission rate and most importantly, based on the energy cost per unit of energy output. The underlying assumption for economic calculations on the gas fuel electrical power plant is that the plant operates at nominal conditions throughout the entire year except for the time of yearly overhaul. Costs of plant components are determined by referring to the nominal operating conditions presented in Table 10.

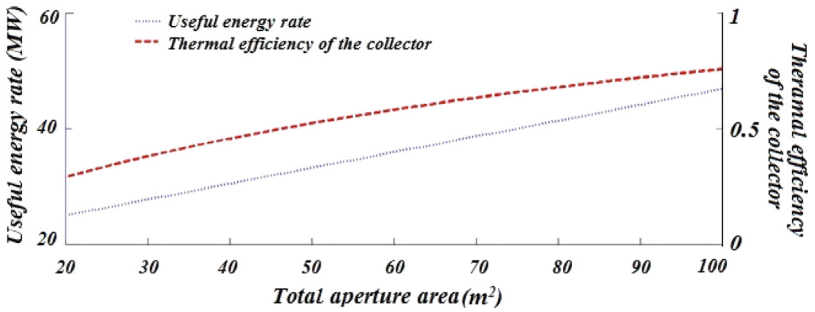

Fig. 13. Variation of the input energy to solar collector receiver and the thermal efficiency of the PTC relative to the total aperture area.

Table 8
Average salary of respective job positions at the PTC electrical power plants.

Cost type	Labor requirement	Salary for single employee (US$/year)
Administration	7	62,857
Operating cost	$N_{operator}$	57,385
Solar field maintenance	$N_{technician}$	55,857

Table 9
The utilized cost elements and assumptions for PTC electrical power plants.

Cost types	Inclusive costs	Estimate	Reference
Direct capital cost			
Site improvements	land preparation, roads, fences, and site infrastructures, such as firewater system, warehouse, and control building	15 US$/m^2	Turchi (2010)
Solar field	Reflective support structures mirrors, tracking system, receiver module, header piping, inter collector piping	295 US$/m^2	Turchi (2010)
HTF system	HTF pumps, solar heat exchangers, HTF expansion, vessel, piping, valves, and instrumentation	90 US$/m^2	Turchi (2010)
Balance of plant	cooling towers, water treatment and storage, electrical, and control systems	7.5% of direct cost	Turchi and Heath (2013)
Contingency	Unaccounted costs in solar field, structures and improvements depending on solar construction site	20% on site improvement, 5% on solar field cost, 10% on storage tank costs	Price (0000)
Decommissioning	Site restoration, environmental fines	5% of the direct cost	Turchi and Heath (2013)
Indirect capital costs			
Sales tax	Tax on non-labor portion of the direct cost upon procurement	No capital acquisition tax	
Operation and maintenance costs			
Equipment and spare parts	Receiver glass replacement, degraded HTF replacement, Heat Exchanger cleaning	0.4% of direct cost/yr.	Price (0000)
Mirror cleaning	Water, cleaning equipment and demineralizing costs	1.1 US$/m^3	Florin and Harris (2008)
Labor	Maintenance personnel, operation controller, field manager, ground keeping,	–	Price (0000)

6.3. Economic and thermodynamic parameters for comparison of powering options

The levelized electricity cost (LCOE) indicates the cost of electricity production for a single kWh of electricity output. The LCOE is given in terms of annualized cost of capital, operation and maintenance cost and fuel cost. In some cases, environmental costs related to emission penalties (CO_2 tax) are calculated on volume or mass basis on the fossil fuel used for energy production are included in determining L_{COE} value. Besides, in order to show the economic effect of the new integrated system, the L_{COE} is calculated as follows (Hong-juan et al., 2013):

$$L_{COE} = \frac{I_{plant} \cdot \times f_{plant\ recovery} + O\ \&\ M_{\frac{annual}{plant}} + FC_{annual+EC}}{E_{elec,output}} \quad (26)$$

Where $I_{plant} \times f_{plant\ recovery}$ is the electrical power plants total investment costs which is including the cost of PTC and installation without considering the costs of land, heat exchangers and the control system, $f_{plant\ recovery}$ is investment cost recovery factor of the electrical power plant, O&M is the annual operating and maintenance expenditure cost, $FC_{annual+EC}$ is annual fuel cost and EC is environmental cost.

The capital investment payback period in refers to the specific period of time which is required to recoup the funds expended in an investment as shown in Fig. 14 (Bellos et al., 2017).

$$\text{Payback period} = \frac{\text{Initial investment}}{\text{Cash inflow per period}} \quad (27)$$

The incremental variation of the solar thermal energy conversion to the electricity efficiency is shown in Fig. 15. (See Table 11.)

Table 10
Cost estimates for 250 MW Rajaee gas power plant.

Cost type	Cost element	Value (MMUS$)
Capital cost	- *Steam Turbine*	257.5
	- *Cost increase due to reheat* piping, valves and controls	
	Heat exchangers	55.63
	Piping	110.7
	Deaerator	1.081
	Condenser	33.94
	Cooling tower	9.565
	Pump	
	- Condenser feed water pump	0.0651
	- Boiler feed pump	0.7793
	- Condenser water pump	0.4188
	Pipe and auxiliary cost	108.1
	Contingencies	18.09
	Land	9.960
	Civil engineering and construction cost	18.09
Operating cost	Coal	104.9
	Maintenance and Spare parts	5.868
	Labor	8.800
	CO_2 tax	33.80
	Environmental tax	67.06

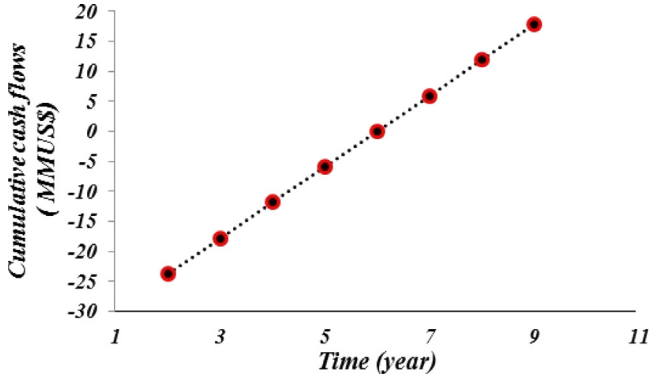

Fig. 14. The cumulative cash flow rates for electrical power boosting mode (120,000 m^2).

Table 11
Economic Input Assumption lists.

Value	Unit	Input parameters
Economic life of solar plant	20	Years
Economic life of coal plant	40	Years
Discount rate	10.5	%
Insurance rate	0.5	%
Escalation rate	2	%
Capital recovery factor for Coal PP	11.2	%
Capital recovery factor for the Solar PP	12.65	%

$$N_{solar\text{-}electricity} = \frac{P_{elec\text{-}power\ cycle} \times \dot{m}_{coal} \times LHV}{P_{solar,\ therm}} \quad (28)$$

7. Conclusions

In this paper, the concept of retrofitting conventional electrical power plant with PTC for various operational modes (increase power and reduce the amount of fuel entering the power plant) and part load status is investigated. It can be pointed that, as the aperture area of solar field increases, annual electrical power generation is increased while specific standard coal consumption decreases. The benefits of the hybrid solar electrical power generation are analyzed in terms of total electrical power output, Rankine cycle thermal efficiency and solar utilization percentage in power boosting mode. The simulations were done for four different sizes of parabolic trough collector. The obtained results show that in a case of using solar thermal energy higher thermal efficiency can be reached compared to the existing electrical power plant. The thermal efficiency when the PTC area equal to 120,000 m^2 is increased from 37% to 39.11%. The electrical power generation for the same scheme is increased to 24 MW when utilization of the solar thermal energy is about 7.0%. The plant operation condition in the fuel saving mode is safer because the electrical power generation value is always below than the rated load and it does not have any effect on the plant safety margins.

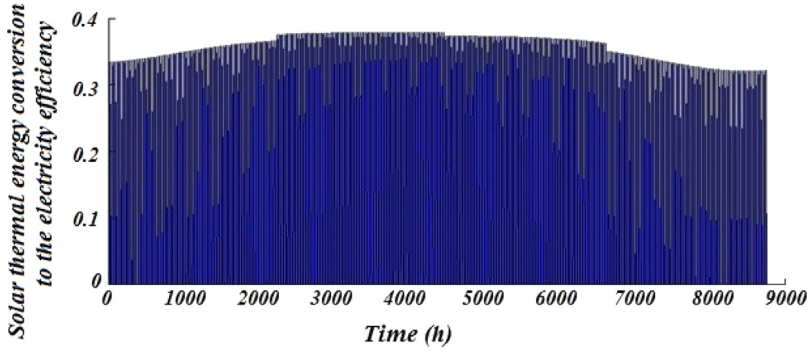

Fig. 15. Variation of solar thermal energy conversion to the electricity efficiency.

In the case of the fuel saving mode, a substantial reduction in the fuel consumption and CO_2 emissions rates is obtained. The annual reductions for a 120,000 m^2 solar collector receiver are 35125.2 ton and 11164.3 ton; respectively. The cost of energy production for electrical power boosting mode is 80 US$/kWh, while this value for the fuel saving mode is 85 US$/MWh. The simple payback period for the electrical power boosting mode is 6 years.

References

Achenbach, E., Riensche, E., 1994. Methane/steam reforming kinetics for solid oxide fuel cells. J. Power Sources 52 (2), 283–288.

Ahmadi, P., Dincer, I., 2010. Exergoenvironmental analysis and optimization of a cogeneration plant system using multimodal genetic algorithm (MGA). Energy 35 (12), 5161–5172.

Ashouri, M., Vandani, A.M.K., Mehrpooya, M., Ahmadi, M.H., Abdollahpour, A., 2015. A techno-economic assessment of a Kalina cycle driven by a parabolic trough solar collector. Energy Convers. Manage. 105, 1328–1339.

Barlev, D., Vidu, R., Stroeve, P., 2011. Innovation in concentrated solar power. Sol. Energy Mater. Sol. Cells 95 (10), 2703–2725.

Bellos, E., Tzivanidis, C., Symeou, C., Antonopoulos, K.A., 2017. Energetic exergetic and financial evaluation of a solar driven absorption chiller — A dynamic approach. Energy Convers. Manage. 137, 34–48.

Chen, Y., Lundqvist, P., Johansson, A., Platell, P., 2006. A comparative study of the carbon dioxide transcritical power cycle compared with an organic rankine cycle with R123 as working fluid in waste heat recovery. Appl. Therm. Eng. 26 (17), 2142–2147.

Costa, M., 2011. Modelling, Simulation and Optimization of Hybrid Solar Power Plants: Solar Augmentation for Coal Fired Power Plants.

Fernández-García, A., Zarza, E., Valenzuela, L., Pérez, M., 2010. Parabolic-trough solar collectors and their applications. Renew. Sustain. Energy Rev. 14 (7), 1695–1721.

Florin, N.H., Harris, A.T., 2008. Enhanced hydrogen production from biomass with in situ carbon dioxide capture using calcium oxide sorbents. Chem. Eng. Sci. 63 (2), 287–316.

Giostri, A., Binotti, M., Astolfi, M., Silva, P., Macchi, E., Manzolini, G., 2012. Comparison of different solar plants based on parabolic trough technology. Sol. Energy 86 (5), 1208–1221.

Hernández-Moro, J., Martínez-Duart, J.M., 2013. Analytical model for solar PV and CSP electricity costs: Present LCOE values and their future evolution. Renew. Sustain. Energy Rev. 20, 119–132.

Hong, H., Peng, S., Zhao, Y., Liu, Q., Jin, H., 2014. A typical solar-coal hybrid power plant in China. Energy Procedia 49, 1777–1783.

Hong-juan, H., Zhen-yue, Y., Yong-ping, Y., Si, C., Na, L., Junjie, W., 2013. Performance evaluation of solar aided feedwater heating of coal-fired power generation (SAFHCPG) system under different operating conditions. Appl. Energy 112, 710–718.

Horn, M., Führing, H., Rheinländer, J., 2004. Economic analysis of integrated solar combined cycle power plants: A sample case: The economic feasibility of an ISCCS power plant in Egypt. Energy 29 (5), 935–945.

Hou, K., Hughes, R., 2001. The kinetics of methane steam reforming over a Ni/α-Al 2 O catalyst. Chem. Eng. J. 82 (1), 311–328.

Hu, E., Yang, Y., Nishimura, A., Yilmaz, F., Kouzani, A., 2010. Solar thermal aided power generation. Appl. Energy 87 (9), 2881–2885.

Kalogirou, S., 2009. Library of Congress Cataloging-in-Publication Data.

Kalogirou, S.A., 2013. Solar Energy Engineering: Processes and Systems. Academic Press.

Kearney, D., Herrmann, U., Nava, P., Kelly, B., Mahoney, R., Pacheco, J., et al., 2003. Assessment of a molten salt heat transfer fluid in a parabolic trough solar field. J. Sol. Energy Eng. 125 (2), 170–176.

Kelly, B., Hermann, U., Hale, M., 2001. Optimization studies for integrated solar combined cycle systems. Sol. Eng. 393–398.

Khaled, A., 2012. Technical and Economic Performance of Parabolic Trough in Jordan. University of Kassel.

Lanhua, D., L., Sufen, 2012. Simulation of hourly solar radiation on tilted surface at Dalian in China. In: 12th International Conference on Clean Energy. Xi'an, China.

Lewis, N.S., Nocera, D.G., 2006. Powering the planet: Chemical challenges in solar energy utilization. Proc. Natl. Acad. Sci. 103 (43), 15729–15735.

Mehrpooya, M., Hemmatabady, H., Ahmadi, M.H., 2015. Optimization of performance of combined solar collector-geothermal heat pump systems to supply thermal load needed for heating greenhouses. Energy Convers. Manage. 97, 382–392.

Mehrpooya, M., Shahsavan, M., Sharifzadeh, M.M.M., 2016a. Modeling energy and exergy analysis of solar chimney power plant-Tehran climate data case study. Energy 115, 257–273.

Mehrpooya, M., Sharifzadeh, M.M.M., 2017. A novel integration of oxy-fuel cycle, high temperature solar cycle and LNG cold recovery–energy and exergy analysis. Appl. Therm. Eng. 114, 1090–1104.

Mehrpooya, M., Sharifzadeh, M.M.M., Rosen, M.A., 2016b. Energy and exergy analyses of a novel power cycle using the cold of LNG (liquefied natural gas) and low-temperature solar energy. Energy 95, 324–345.

Montes, M., Abánades, A., Martinez-Val, J., Valdés, M., 2009. Solar multiple optimization for a solar-only thermal power plant, using oil as heat transfer fluid in the parabolic trough collectors. Sol. Energy 83 (12), 2165–2176.

Montes, M., Rovira, A., Muñoz, M., Martínez-Val, J., 2011. Performance analysis of an integrated solar combined cycle using direct steam generation in parabolic trough collectors. Appl. Energy 88 (9), 3228–3238.

Moradi, M., Mehrpooya, M., 2017. Optimal design and economic analysis of a hybrid solid oxide fuel cell and parabolic solar dish collector, combined cooling, heating and power (CCHP) system used for a large commercial tower. Energy 130, 530–543.

Muñoz, J., Abánades, A., Martínez-Val, J.M., 2009. A conceptual design of solar boiler. Sol. Energy 83 (9), 1713–1722.

Niknia, I., Yaghoubi, M., 2012. Transient simulation for developing a combined solar thermal power plant. Appl. Therm. Eng. 37, 196–207.

Niknia, I., Yaghoubi, M., 2013. Transient analysis of integrated Shiraz hybrid solar thermal power plant. Renew. Energy 49, 216–221.

Peng, S., Hong, H., Wang, Y., Wang, Z., Jin, H., 2014. Off-design thermodynamic performances on typical days of a 330 MW solar aided coal-fired power plant in China. Appl. Energy 130, 500–509.

Popov, D., 2011. An option for solar thermal repowering of fossil fuel fired power plants. Sol. Energy 85 (2), 344–349.

Price, H., 0000. A parabolic trough solar power plant simulation model. In: Conference A parabolic trough solar power plant simulation model. American Society of Mechanical Engineers, pp. 665–73.

Raj, N.T., Iniyan, S., Goic, R., 2011. A review of renewable energy based cogeneration technologies. Renew. Sustain. Energy Rev. 15 (8), 3640–3648.

Sabziparvar, A.A., 2008. A simple formula for estimating global solar radiation in central arid deserts of Iran. Renew. Energy 33 (5), 1002–1010.

Shahin, M.S., Orhan, M.F., Uygul, F., 2016. Thermodynamic analysis of parabolic trough and heliostat field solar collectors integrated with a Rankine cycle for cogeneration of electricity and heat. Sol. Energy 136, 183–196.

Shimeles, S., 2014. Thermo-Economic Analysis of Retrofitting an Existing Coal-Fired Power Plant with Solar Heat (Student thesis).

Soteris, K., 2009. Solar Energy Engineering-Processes and Systems. Elsevier Academic Press UK.

Spelling, J., Russ, M., Laumert, B., Fransson, T., 0000. A thermoeconomic study of hybrid solar gas-turbine power plants. In: Conference A Thermoeconomic Study of Hybrid Solar Gas-Turbine Power Plants.

Steinfeld, A., Palumbo, R., 2001. Solar thermochemical process technology. Encycl. Phys. Sci. Technol. 15 (1), 237–256.

Suresh, M., Reddy, K., Kolar, A.K., 2010. 4-E (energy, exergy, environment, and economic) analysis of solar thermal aided coal-fired power plants. Energy Sustain. Dev. 14 (4), 267–279.

Turchi, C.S., 2010. Parabolic Trough Reference Plant for Cost Modeling with the Solar Advisor Model (SAM). Citeseer.

Turchi, C.S., Heath, G.A., 2013. Molten salt power tower cost model for the system advisor model (SAM). Contract 303, 275–3000.

Van Sciver, S.W., 2011. Helium Cryogenics, second ed. Springer Science & Business Media.

Yang, Y., Yan, Q., Zhai, R., Kouzani, A., Hu, E., 2011. An efficient way to use medium-or-low temperature solar heat for power generation–integration into conventional power plant. Appl. Therm. Eng. 31 (2), 157–162.

Ying, Y., Hu, E.J., 1999. Thermodynamic advantages of using solar energy in the regenerative Rankine power plant. Appl. Therm. Eng. 19 (11), 1173–1180.

Zhao, Y., Hong, H., Zhang, X., Jin, H., 2012. Integrating mid-temperature solar heat and post-combustion CO2-capture in a coal-fired power plant. Sol. Energy 86 (11), 3196–3204.